A study of respiration-correlated cone-beam CT scans to correct target positioning errors in radiotherapy of thoracic cancer

J. P. Santoro,[a] J. McNamara, E. Yorke, and H. Pham
Department of Medical Physics, Memorial Sloan Kettering Cancer Center, New York, New York 10065

A. Rimner and K. E. Rosenzweig[b]
Department of Radiation Oncology, Memorial Sloan Kettering Cancer Center, New York, New York 10065

G. S. Mageras[c]
Department of Medical Physics, Memorial Sloan Kettering Cancer Center, New York, New York 10065

(Received 10 January 2012; revised 10 August 2012; accepted for publication 13 August 2012; published 11 September 2012)

Purpose: There is increasingly widespread usage of cone-beam CT (CBCT) for guiding radiation treatment in advanced-stage lung tumors, but difficulties associated with daily CBCT in conventionally fractionated treatments include imaging dose to the patient, increased workload and longer treatment times. Respiration-correlated cone-beam CT (RC-CBCT) can improve localization accuracy in mobile lung tumors, but further increases the time and workload for conventionally fractionated treatments. This study investigates whether RC-CBCT-guided correction of systematic tumor deviations in standard fractionated lung tumor radiation treatments is more effective than 2D image-based correction of skeletal deviations alone. A second study goal compares respiration-correlated vs respiration-averaged images for determining tumor deviations.

Methods: Eleven stage II–IV nonsmall cell lung cancer patients are enrolled in an IRB-approved prospective off-line protocol using RC-CBCT guidance to correct for systematic errors in GTV position. Patients receive a respiration-correlated planning CT (RCCT) at simulation, daily kilovoltage RC-CBCT scans during the first week of treatment and weekly scans thereafter. Four types of correction methods are compared: (1) systematic error in gross tumor volume (GTV) position, (2) systematic error in skeletal anatomy, (3) daily skeletal corrections, and (4) weekly skeletal corrections. The comparison is in terms of weighted average of the residual GTV deviations measured from the RC-CBCT scans and representing the estimated residual deviation over the treatment course. In the second study goal, GTV deviations computed from matching RCCT and RC-CBCT are compared to deviations computed from matching respiration-averaged images consisting of a CBCT reconstructed using all projections and an average-intensity-projection CT computed from the RCCT.

Results: Of the eleven patients in the GTV-based systematic correction protocol, two required no correction, seven required a single correction, one required two corrections, and one required three corrections. Mean residual GTV deviation (3D distance) following GTV-based systematic correction (mean $\pm$ 1 standard deviation 4.8 $\pm$ 1.5 mm) is significantly lower than for systematic skeletal-based (6.5 $\pm$ 2.9 mm, $p = 0.015$), and weekly skeletal-based correction (7.2 $\pm$ 3.0 mm, $p = 0.001$), but is not significantly lower than daily skeletal-based correction (5.4 $\pm$ 2.6 mm, $p = 0.34$). In two cases, first-day CBCT images reveal tumor changes—one showing tumor growth, the other showing large tumor displacement—that are not readily observed in radiographs. Differences in computed GTV deviations between respiration-correlated and respiration-averaged images are 0.2 $\pm$ 1.8 mm in the superior-inferior direction and are of similar magnitude in the other directions.

Conclusions: An off-line protocol to correct GTV-based systematic error in locally advanced lung tumor cases can be effective at reducing tumor deviations, although the findings need confirmation with larger patient statistics. In some cases, a single cone-beam CT can be useful for assessing tumor changes early in treatment, if more than a few days elapse between simulation and the start of treatment. Tumor deviations measured with respiration-averaged CT and CBCT images are consistent with those measured with respiration-correlated images; the respiration-averaged method is more easily implemented in the clinic. [http://dx.doi.org/10.1118/1.4748503]

Key words: cone-beam computed tomography, image-guided radiation treatment, organ motion, lung cancer

I. INTRODUCTION

Although image guidance of radiation therapy is rapidly evolving, the traditional and still commonly used method for correcting setup error in radiation therapy treatments is weekly comparison of bony anatomy as visualized in an orthogonal pair of plain radiographs (kV or MV) to a corresponding pair of digitally reconstructed radiographs (DRRs) or radiographs from the simulation. As examples, the recently closed RTOG protocol 0617 requires weekly verification or orthogonal images to be taken,[1] and the currently active RTOG protocol 1106 lists orthogonal kV or MV 2D images as acceptable pretreatment image types.[2] Because tumors are often poorly visualized on these images, there is increasingly widespread use of cone-beam CT (CBCT) for guiding radiation treatment, especially in lung cancer where soft tissue contrast in lung facilitates gross tumor volume (GTV) visualization.[3–11] References 3–8, and 10 have examined single or few-fraction treatments. Yeung *et al.*,[9] Bissonnette *et al.*,[10] and Wang *et al.*[11] have used daily CBCT and soft tissue registration to correct patient position in treatments of 20 or more sessions. Challenges associated with daily CBCT-guided correction of such conventionally fractionated treatments include imaging dose to the patient (~2–5 cGy/scan to soft tissue, higher to bone).[12] Daily image guidance, whether CBCT or orthogonal kV radiographs, entails increased workload and treatment time associated with imaging system setup, image acquisition, image registration, and position correction (at least 5 min per treatment).

Patient correction from cone-beam CT-based measurements acquired in the first few treatment fractions can correct for systematic error in GTV position arising from differences between simulation and treatment. In so-called off-line protocols, systematic error is determined from several measurements and corrected in subsequent treatment fractions. In a study of interfractional variations in lung tumor position using megavoltage CBCT, systematic deviations were comparable or larger than random ones, suggesting that using volumetric imaging for correction of systematic error could be an efficient and effective means of improving treatment accuracy.[13]

A particular challenge in thoracic disease sites is that respiratory motion can introduce artifacts in a planning CT scan and blur in a CBCT, thus reducing localization accuracy. Respiration-correlated CT (RCCT), where images are retrospectively binned according to the respiratory phase, has been shown to reduce respiratory motion artifacts and yield 3D images at different points in the respiratory cycle.[14–17] In a similar approach, respiration-correlated CBCT (RC-CBCT) uses retrospective binning of projection images according to respiration.[3,18–20] For both simulation (RCCT) and image-guided treatment (RC-CBCT), these techniques allow the GTV position to be more precisely localized in each of the phase-binned image sets, owing to the reduced motion within each bin. This yields a tumor trajectory that can be compared to a chosen reference phase, e.g., end-expiration or mid-inspiration. RC-CBCT provides more information than conventional CBCT but requires longer acquisition and processing times and, at present, software that is less widely available.

We report here on a prospective patient study in which RC-CBCT guidance was used in an off-line protocol to correct for systematic errors in GTV position in standard fractionated treatment of later stage lung cancer. As mentioned above, correction of systematic error can be an effective means of improving targeting accuracy. However, the protocol is labor-intensive, costly in terms of longer treatment sessions and currently unavailable on many linacs, including most of those at our institution. We report here on an examination of the efficacy of the method through analysis of the acquired images. Specifically, we examine two questions. The first is whether a CBCT-guided protocol to correct systematic deviations in advanced stage lung tumors is more effective than radiograph-based protocols that correct skeletal deviations alone. The second question is whether planning RCCT and RC-CBCT in these types of treatments yield different corrections for GTV position than do respiration-averaged CT and CBCT.

II. METHODS AND MATERIALS

This study is part of an IRB-approved protocol which enrolled eleven patients with stage II–IV, nonsmall cell lung cancer (NSCLC). All patients had tumor attached to the mediastinum, and 9 of 11 have additional tumor in lung. In all cases, lung-soft tissue contrast allowed for visualization of some parts of the GTV on all scans. The visible portion was in the upper lung in seven patients, middle lung in two patients, and lower lung in two patients. The range of GTV volumes attached to the mediastinum was 40–290 cm^3 and the range of GTV in lung was 5–73 cm^3. Each patient received an RCCT at simulation (Light Speed, GE Health Care, Waukesha, WI) with breathing recorded by an external monitor (Real-time Position Management (RPM), Varian Medical Systems, Palo Alto, CA). A conventional helical CT scan for treatment planning purposes was acquired at the same session. No special breathing control methods were used for either scan. The RCCT images were binned into ten respiratory phases using the vendor's software (Advantage 4D) with 0% denoting end-inspiration (EI) and 50% approximate end expiration (EE) as determined from the external monitor; for some patients, the point of superior-most diaphragm position, representing EE, was closer to 60%. For this study, a single physician (K.R.) delineated the GTV on the 50% image set. For treatment planning, the physician used the RCCT to define an internal target volume (ITV) encompassing the GTV at all phases. The ITV was expanded form the clinical target volume (CTV) which is further expanded to form the planning target volume (PTV). All patients were simulated and treated with the 6 MV beam of a Trilogy Linac (Varian Medical Systems) in customized alpha-cradle immobilization with no special breathing control methods in place. The prescribed dose per fraction (1 fraction/day) was 2 Gy ($n = 10$) and 1.8 Gy ($n = 1$) with total doses ranging from 45 to 70 Gy. One patient was treated with 3D conformal radiotherapy (3D-CRT), the

others were delivered with intensity-modulated radiotherapy (IMRT).

The prospective interventional study uses an off-line protocol to correct for systematic deviations in GTV position. For the first five treatment days, the patient is set up conventionally by aligning skin-marks placed at simulation to room lasers and corrected by couch shifts determined from orthogonal radiographs acquired prior to the first treatment. In addition, each patient receives an RC-CBCT scan immediately before treatment on the first 5 days of treatment and a correction, if needed (described below) is applied on the sixth fraction. To account for possible trends in GTV position in the remainder of the treatment course, an RC-CBCT scan is acquired every fifth treatment day thereafter, a systematic deviation is computed using a running average of the five most recent RC-CBCT scans, and a correction, if needed, is applied the following fraction. The RC-CBCT scan, together with the RCCT at simulation, is used to compute the respiration motion trajectory of the GTV and to correct for its motion-averaged position. The RC-CBCT scan uses a kilovoltage x-ray imaging system (On-Board Imaging, Varian Medical Systems), which has been described in detail in Ref. 21.

To acquire an RC-CBCT scan, the gantry rotation speed is reduced to 0.2 rpm using research software provided by the vendor. The reduced gantry speed increases the number of projections acquired and reduces gaps in projections between respiratory cycles in the phase-binned image sets. The choice of gantry speed is a trade-off between scan duration and reconstructed image quality. The full-fan scan (detector centered on the x-ray central axis) is acquired over an angle of $\sim 200^\circ$ instead of the full 360°, to reduce the scan time (2.8 min) and imaging dose. Acquisition rate is 11 images/s, yielding a total of approximately 1800 projection images per scan. The reconstructed scan diameter is 25 cm. The exposure (mA-s) settings are also reduced so that the dose per scan is the same as for a standard CBCT (2 cGy to center, 4 cGy to skin). During each RC-CBCT scan, the respiration trace is recorded using the RPM system. Specially designed circuitry provided by the vendor for research purposes provides an x-ray on-off signal, which is recorded simultaneously with the RPM signal. A research software application provided by Varian tags each projection image with its respiration phase. Custom software written at this institution sorts the RC-CBCT images into user-defined respiratory phase bins. Six respiratory bins are used, centered at phases 0% (end-inspiration), 16%, 32% (mid-expiration), 50% (end-expiration), 66%, and 82% (mid-inspiration). Each bin is reconstructed (filtered back-projection algorithm, Varian research software Viva rev. K.04) to yield an RC-CBCT image set. The choice of six bins is a trade-off between acceptable reconstructed CBCT image quality and residual motion within each bin (Figure 1 shows an example RC-CBCT image set). Each bin contains an approximately equal number (300) of projections, thus representing approximately equal time-weighted bins for computing the GTV motion trajectory and respiration-averaged position (described below). An additional reconstruction is performed using all of the $\sim$1800 projections in the scan, to yield a respiration-averaged CBCT.

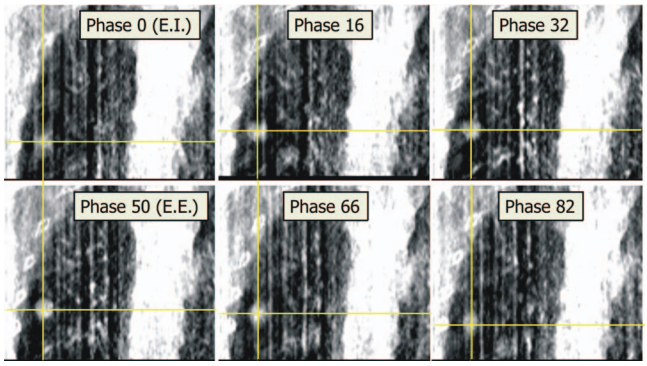

FIG. 1. Coronal section from six phase-binned images of a respiration-correlated cone-beam CT (RC-CBCT) scan of Patient 4. Tumor is shown at cross hairs in each phase.

The six RC-CBCT and ten RCCT image sets are used to determine the deviation of the respiration-averaged position of the tumor centroid from the planned position. This is done in four steps: (1) The tumor motion trajectory in the RCCT, i.e., displacement of the tumor from end expiration, is determined in each of the other nine images using rigid image registration (translations only) to visually align the GTV in the two overlaid images. The average of ten displacements (including the zero displacement at end expiration) gives the respiration-averaged position relative to the end-expiration position. (2) In the same way, the motion trajectory and respiration-averaged tumor position in the RC-CBCT is determined relative to its end-expiration position, by registering the end-expiration image to each of the other five images in the set. Figure 2 shows the GTV trajectories from the RCCT and RC-CBCT images of Patient 11. (3) The displacement of the tumor at end-expiration in the RC-CBCT is

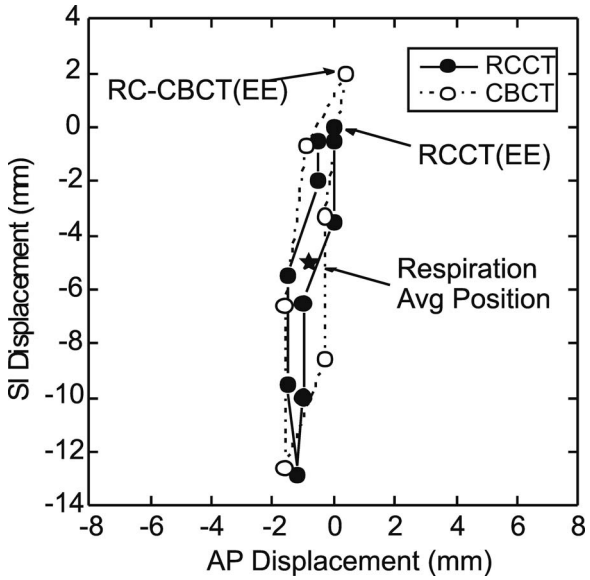

FIG. 2. Example tumor trajectories in the anterior-posterior (A/P) and superior-inferior (S/I) directions, obtained from the respiration-correlated CT (RCCT) and one of the respiration-correlated cone-beam CT (RC-CBCT) image sets of Patient 11. Each point indicates displacement relative to the 50% phase reference point (approximately end expiration, EE) in the RCCT. Star symbol indicates the respiration average position in both image sets.

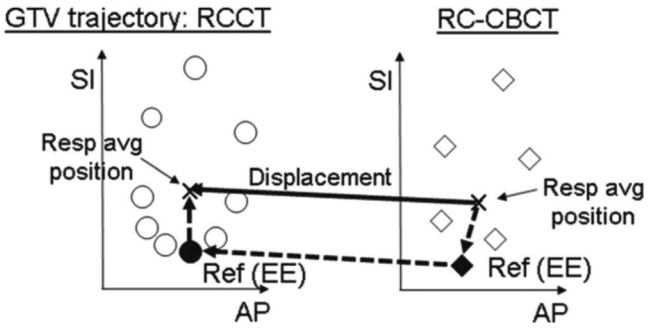

FIG. 3. Graphical representation of procedure used to determine the displacement of the respiration-averaged gross tumor volume (GTV) position ("Resp avg position") in the respiration-correlated cone-beam CT (RC-CBCT) relative to that in the respiration-correlated CT (RCCT). Circle and diamond symbols denote the GTV trajectory along anterior-posterior (AP) and superior-inferior (SI) directions in the RCCT and RC-CBCT image sets, respectively. Displacement of the respiration-averaged GTV (solid arrow) is derived from the sum of three vectors (dashed arrows): the displacement of the respiration-averaged GTV from the end-expiration ("Ref EE") in the reference RCCT image; the corresponding displacement in the RC-CBCT; and displacement of the GTV at EE in the RC-CBCT relative to its EE position in the RCCT.

determined relative to the end-expiration RCCT, using rigid image registration. The RCCT and RC-CBCT are initially aligned to the isocenter in the two images, corresponding to zero displacement. (4) A vector addition of the above three displacements is performed (Fig. 3), to yield the deviation of the respiration-averaged tumor position in the RC-CBCT from its position in the RCCT. The above analysis is computed using custom software developed at this institution.

The accuracy of the above respiration-correlated procedure is tested in phantom. A motion phantom (Quasar, Modus Medical Devices, London, ON) is programmed to follow a patient respiratory trace. The trace exhibits a longer quiescent portion at end expiration than at end inspiration, which is typical of patient respiration and serves as a test of calculating the respiration-averaged tumor position. A 20 mm spherical object embedded in acrylic and with peak-to-trough motion extent of 12 mm along the axial direction is used as a mock tumor. RCCT and RC-CBCT scans are acquired of the phantom programmed with the same respiration trace, thus the respiration-averaged tumor position is expected to be the same in both scans. The procedure described in the previous paragraph is followed to compute the deviation of the respiration-averaged tumor position in the RC-CBCT relative to the RCCT. To remove setup uncertainty of the phantom in the two scans, the RC-CBCT and RCCT scans are registered to the stationary portion of the phantom and this deviation is subtracted. The resultant tumor deviation is 1.3, 0.1, and 0.8 mm in the lateral, vertical, and axial (phantom motion) directions, respectively, consistent with the expected null result to within the repeatability of the registration procedure (approximately 1 mm in each direction). We note that the lateral dimension of the phantom is larger than the CBCT reconstruction field-of-view, thus slightly increasing the error in the registration to the stationary portion of the phantom in that direction.

II.A. Comparison of correction protocols

To answer the first study question, i.e., whether a CBCT-guided protocol to correct systematic GTV deviations is more effective than radiograph-guided correction, we compare the following correction methods:

- Type 1: Correct for systematic error in GTV position using RCCT and RC-CBCT. This correction method is used for the patient treatments.
- Type 2: Correct for systematic error in bony (vertebral column) anatomy using orthogonal planar images. This assumes the same timing as correction method 1 but determines shifts using the vertebral column rather than the GTV.
- Type 3: Daily correction of vertebral column displacements using orthogonal planar images. This corrects both systematic and random setup errors.
- Type 4: Weekly correction of vertebral column displacements using orthogonal planar images.

The other types of corrections (Types 2–4) were not used in this protocol, but they make use of the acquired images to study the added value of a correction based on RC-CBCT imaging relative to one based on skeletal anatomy (i.e., based on radiographs).

We describe the calculation of Type 1 corrections. We define $T_{g,i}$ as the translation which aligns the respiration-averaged GTV position in the ith RC-CBCT scan to the respiration-averaged GTV position in the RCCT. In the first five scans ($i = 1, 2, \ldots, 5$) the patient (hence the CBCT isocenter) is positioned according to the skin tattoos plus shifts determined from radiographs on the day prior to the first treatment. In subsequent scans ($i = 6, 7, \ldots$) the CBCT isocenter is corrected for systematic error in GTV position as described below. The systematic correction in GTV position is calculated from the previous five scans as

$$\bar{T}_{g,i} = \frac{1}{5}\sum_{j=i-5}^{i-1} T_{g,j}, (i = 6),$$

$$\bar{T}_{g,i} = \frac{1}{5}\sum_{j=i-5}^{i-1} (T_{g,j} + \bar{T}_{g,j}), (i > 6), \quad (1)$$

and $\bar{T}_{g,i} = (0, 0, 0)$ for $i = 1, 2, \ldots, 5$. Note that for $i > 6$ the additional term $\bar{T}_{g,j}$ accounts for the different positioning of the isocenter in different CBCT scans as described above. If the correction $\bar{T}_{g,i}$ differs by 3 mm or more in any of the three principal directions from the previous correction $\bar{T}_{g,i-1}$, it is applied in that direction at the ith CBCT scan (for $i \geq 6$); otherwise the previous correction is retained. This is to avoid large numbers of changes in correction and associated increased workload. In the actual treatment protocol, the first correction is applied to treatment fractions 6–10 as well as to the CBCT scan at the 10th fraction ($i = 6$).Following the 10th fraction, $\bar{T}_{g,7}$ is computed, and if it differs by 3 mm or more from $\bar{T}_{g,6}$, a new correction is applied to fractions 11–15 and to the CBCT scan at the 15th fraction ($i = 7$), and so on until treatment course completion. The clinical process

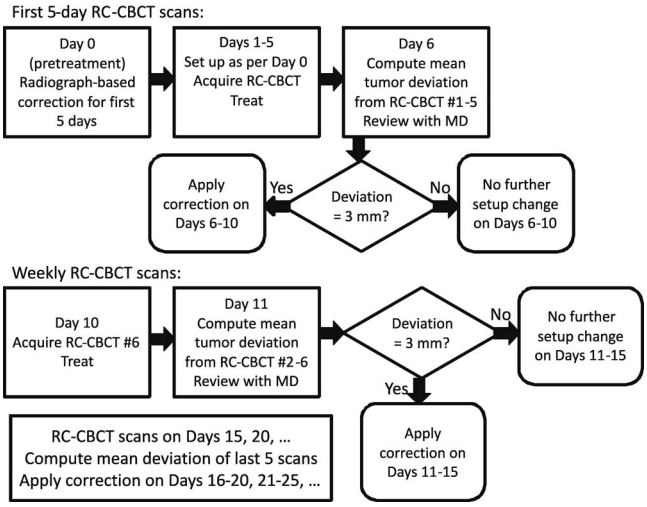

FIG. 4. Flow chart of the clinical RC-CBCT guided (Type 1) correction process.

is summarized in Figure 4. For the purposes of retrospective comparison in this study, we consider GTV deviations only on those days when a CBCT scan has occurred to provide information.

The other correction methods are retrospectively simulated using the scans acquired during the clinical protocol, for which Type 1 correction is used. In the calculation of Type 2 corrections, $T_{b,i}$ is the translation which aligns the vertebral column in the ith RC-CBCT scan to the planning CT, which is acquired with the patient in the same position as the RCCT. The values are obtained from registrations of sagittal and coronal sections between the CBCT scan using all projections (which gives better visualization of bone than single phase-binned image sets) and the RCCT. For the purposes of this study the corrections are assumed to represent orthogonal radiograph-based corrections. For $i = 1$–5 the scans are acquired daily, whereas for $i = 6$, 7, etc. they occur at weekly intervals. The systematic correction to bony anatomy is given by

$$\bar{T}_{b,i} = \frac{1}{5}\sum_{j=i-5}^{i-1} T_{b,j}, (i = 6),$$

$$\bar{T}_{b,i} = \frac{1}{5}\sum_{j=i-5}^{i-1} (T_{b,j} + \bar{T}_{g,j}), (i > 6). \quad (2)$$

This is applied at the ith CBCT scan and determined from the previous five scans. As in Eq. (1), the term $\bar{T}_{g,j}$ in Eq. (2) accounts for the isocenter positioning in the CBCT scans according to the tumor-based correction that is used in patient treatments and therefore affects the CBCT isocenter for $i > 6$. Similarly to the Type 1 correction, if the Type 2 correction $\bar{T}_{b,i}$ differs by 3 mm or more in any direction from the previous correction, it is applied, but only in that direction; otherwise the previous correction is retained.

To simulate daily bony-based corrections (Type 3), the correction $T_{b,i}$ obtained from the ith CBCT scan is applied to the data from the same scan. In Type 4 corrections, $T_{b,i}$ obtained from the ith scan is applied to the data from the $(i + 1)$th scan, to simulate the effect of weekly bony corrections on nonmeasurement days. For both types of corrections, registration of sagittal and coronal sections between the CBCT and RCCT are assumed to represent orthogonal radiograph-based corrections.

We compare the residual error in GTV position for the different correction methods. We refer to residual error as the deviation in GTV from the planned position following application of a correction. For scans 6, 7, 8, etc., the residual error δ_i^{T1} after the (Type 1) correction of systematic GTV deviation $\bar{T}_{g,i}$ is applied is given by

$$\delta_i^{T1} = -T_{g,i}, (i \geq 1), \quad (3)$$

where the superscript indicates the type of correction. It is in effect a measure of the daily random patient setup (i.e., bony anatomy positioning), random GTV deviations relative to the bony anatomy, and any residual systematic deviation owing to the uncertainty in its estimate from five measurements. Note that for scans 1–5, Eq. (3) also applies.

The residual error in GTV position δ_i^{T2} after a (Type 2) correction $\bar{T}_{b,i}$ of systematic error in bony anatomy is applied is given by

$$\delta_i^{T2} = -T_{g,i}, (i \leq 5),$$

$$\delta_i^{T2} = -(T_{g,i} + \bar{T}_{g,i} - \bar{T}_{b,i}), (i \geq 6). \quad (4)$$

For scans 1–5 the residual error is the same as for Type 1 corrections. For scans 6 and higher, the residual error is calculated retrospectively by removing the GTV-based correction of systematic error $\bar{T}_{g,i}$ then applying the bony-based systematic correction $\bar{T}_{b,i}$.

The residual error in the GTV position δ_i^{T3} after a (Type 3, retrospectively simulated) daily correction for bony anatomy is obtained for the ith (current) scan is

$$\delta_i^{T3} = -(T_{g,i} - T_{b,i}), (i \leq 5, i \geq 6). \quad (5)$$

The residual error in GTV position after a (Type 4, retrospectively simulated) weekly correction for bony anatomy obtained only from the prior scan from a week ago [i.e., the $(i-1)$th scan] is

$$\delta_i^{T4} = -T_{g,i}, (i \leq 5),$$

$$\delta_i^{T4} = -[T_{g,i} + \bar{T}_{g,i} - (T_{b,i-1} + \bar{T}_{g,i-1})], (i \geq 6), \quad (6)$$

where $T_{b,i-1}$ is the $(i-1)$th bony based correction.

For all type corrections, the mean residual error is computed as a weighted average of the residual errors δ_i on scan days. Since the first five scans occur daily whereas subsequent scans occur weekly, in order to estimate the mean residual error over the treatment course, the first five measurements are weighted by one-fifth relative to the subsequent measurements.

II.B. Comparison respiration-correlated versus respiration-averaged image registration

To address the second question in this study, we compare the Type 1 respiration-correlated image-based registration (Fig. 3) with respiration-averaged image-based registration.

In the latter, we construct a respiration-averaged reference image by computing an average intensity projection from the RCCT scan (AVE-IP) using the vendor's software. For each RC-CBCT scan acquired, we reconstruct a single CBCT image using all ~1800 projection images, yielding an effectively respiration-averaged scan. The tumor in the respiration-averaged CBCT is registered to the tumor in the AVE-IP using the in-house registration software to yield a differently implemented measurement of the respiration-averaged deviation in tumor position. For each scan, the tumor position as determined by the respiration-correlated method T_{RC} is compared to the tumor position as determined by the respiration-averaged method T_{RA}. The number of CBCT scans for each of the 11 patients ranged from 7 to 11 for a total of 103 scans. The difference $T_{RA} - T_{RC}$ is computed for each of the 105 scans comprising the 11-patient cohort.

As a check of the respiration-averaged registration procedure, the previously described RCCT and RC-CBCT scans of the motion phantom are used to generate an AVE-IP CT and CBCT image using all projections. Two registrations are performed, the first to align the mock tumor, the second to align the stationary portion of phantom, and the difference in registrations computed to remove setup uncertainty. The resultant deviation is 1.0, 0.4, and 0.2 mm in the lateral, vertical, and axial (phantom motion) directions, consistent with the expected null result to within the repeatability of the registration.

III. RESULTS

Figure 5 shows an example of the GTV 3D deviations for Patient 1, on those treatment fractions in which an RC-CBCT scan was acquired. The data labeled "GTV systematic" are the actual measurements resulting from the RC-CBCT guided correction (Type 1) used in the patient study, whereas the data for the other correction methods are retrospectively simulated as described in Sec. II. In this case a single correction of 7 mm (inferior shift of the patient) was applied to fractions 6 and thereafter. No further corrections were required as subsequent Type 1 deviations were below the 3 mm action level. One can see that the 3D deviation prior to the Type 1 correction (fractions 1–5) varies between 4 and 10 mm, whereas after correction (fractions 10–25) the residual deviation varies between 2 and 4 mm. In the bony-based systematic (Type 2) and bony-based weekly (Type 4) methods, corrections are made following fraction 5, hence the deviations in fractions 1–5 are the same as those for Type 1. In fractions 10–25, Type 2 and Type 4 corrections result in larger residual deviations than with Type 1. In the bony-based daily (Type 3) method, correction is made at each fraction, hence the deviations in fractions 1–5 differ from the other correction methods. In fractions 10–25, residual deviations with Type 3 corrections are larger than with Type 1 but generally smaller than with Type 2 and Type 4 corrections.

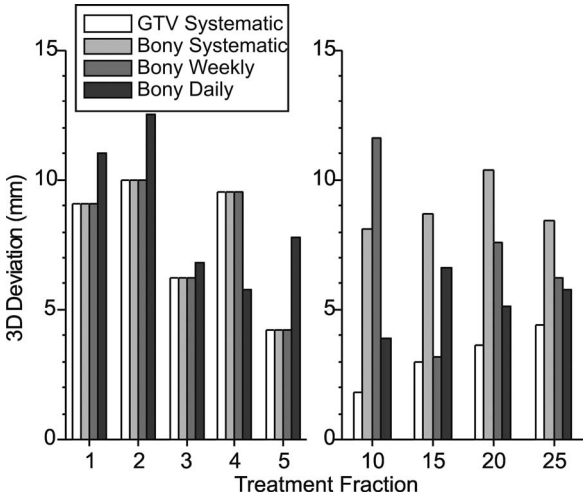

FIG. 5. Example (Patient 1) of 3D deviations in GTV position on treatment fractions in which an RC-CBCT scan was acquired. Data labeled "GTV systematic" are the actual measurements resulting from the RC-CBCT guided (Type 1) correction shown in Fig. 4, whereas data for the other correction methods are retrospectively simulated as described in the text.

III.A. Comparison of correction protocols

Of the eleven patients that completed the study with GTV-based systematic (Type 1) corrections, two required no correction, seven required a single correction (after scan 5), one required two corrections (after scans 5 and 7), and one required three corrections (after scans 5, 7, and 8). Figure 6 shows the mean 3D residual errors and 1-standard-deviation (1SD) error bars for the four correction methods. The GTV-based systematic error correction yields lower residual errors in 9 out of 11 cases relative to bony-based systematic (Type 2) correction, in 6/11 cases relative to bony-based daily (Type 3) correction, and in 10/11 cases relative to bony-based based weekly (Type 4) correction. Mean ± 1SD 3D residual error (over measurements and patients) in GTV-based systematic correction (4.8 ± 1.5 mm) is lower than for systematic bony-based correction (6.5 ± 2.9 mm), daily bony-based correction (5.4 ± 2.6 mm), and weekly bony-based correction (7.2 ± 3.0 mm). A paired 2-tailed *t*-test of significance shows that GTV-based systematic correction yields significantly lower

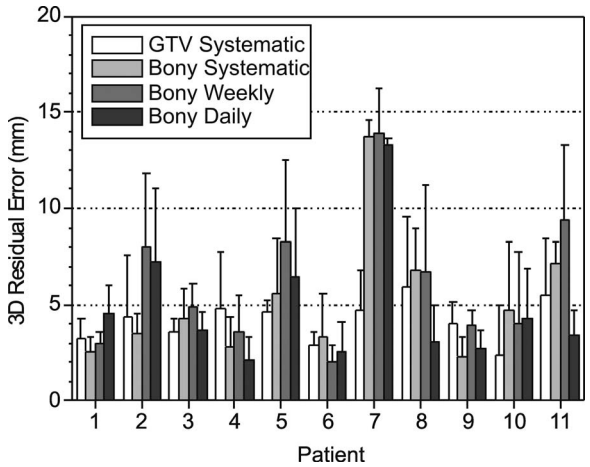

FIG. 6. Mean 3D residual GTV position errors of GTV-based systematic (Type 1) correction, bony-based systematic (Type 2) correction, bony-based daily (Type 3) correction, and bony-based weekly (Type 4) correction versus patient. Error bars indicate 1-standard-deviation residual error.

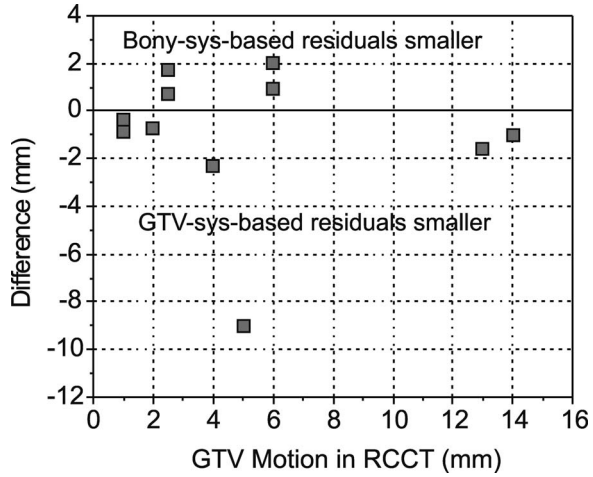

FIG. 7. Difference in mean GTV residual error between GTV-based systematic (Type 1) and bony-based systematic (Type 2) corrections, vs GTV motion extent in RCCT.

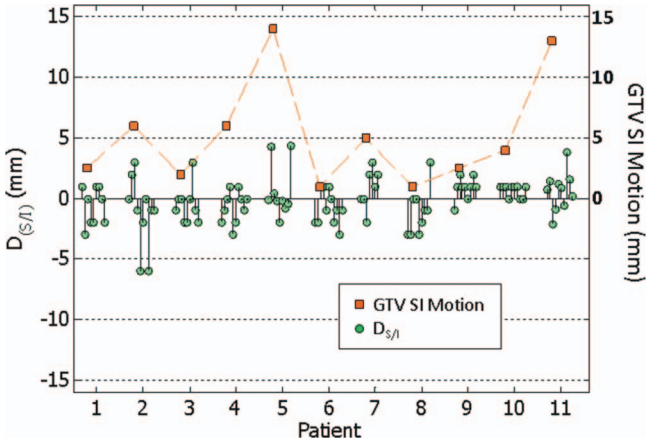

FIG. 8. Difference in GTV superior-inferior displacement $D_{S/I}$ between respiration-correlated (RCCT-to-RC-CBCT) and respiration-averaged (AVE-IP-to-CBCT using all projections) image registration (circle symbols). Square symbols indicate maximum S/I displacement of the GTV from its end-expiration position in the RCCT scan.

residual error relative to bony-based systematic ($p = 0.015$) and bony-based weekly corrections ($p = 0.001$) but is not significant relative to bony-based daily corrections ($p = 0.34$). Patients 1 and 7 show the largest benefit with GTV-based systematic correction and are discussed further below.

We examine whether differences between GTV-based and bony-based correction are more pronounced with larger respiration-induced tumor motion. Figure 7 plots the difference in 3D residual error (GTV-based systematic minus bony-based systematic correction) versus GTV motion extent (end-expiration to end-inspiration) as determined from the RCCT. There is no significant correlation. One sees that the difference in residual error is less than 2 mm in 9/11 cases. We note that tumor motion extent is 6 mm or less in 9/11 cases.

III.B. Comparison of respiration-correlated versus respiration-averaged image registration

Figure 8 shows the difference in GTV SI displacement between respiration-averaged (AVE-IP-to-CBCT using all projections) and respiration-correlated (RCCT-to-RC-CBCT) image registration $T_{RA} - T_{RC}$. The figure also shows the motion extent in the SI direction from the RCCT at simulation. The mean ± 1SD difference for 11 patients (103 CBCT scans) is –0.1 ± 1.8 mm (L/R), 0.0 ± 2.0 mm (A/P), and 0.2 ± 1.8 mm (S/I). There is a small correlation between S/I difference (data points denoted by circles) and S/I motion extent ($r = 0.20$) but with marginal statistical significance ($p = 0.05$).

III.C. Incidental finding

In two cases the first-day CBCT revealed tumor changes that were not readily observed in radiographs. In Patient 1 (Fig. 9) the first-day CBCT, acquired 19 days after simulation, showed growth of the GTV beyond the GTV boundaries at simulation, which led to a change in the treatment plan. In Patient 7, (Fig. 10) the first-day CBCT was 12 days after simulation, and showed that part of the GTV in lung had shifted posteriorly by approximately 14 mm. This also led to a change in the treatment plan.

IV. DISCUSSION AND CONCLUSIONS

In this study, we applied an off-line protocol for setup correction of patients being treated with conventional fractionation for locally advanced NSCLC, based on changes in the average displacement of the GTV as observed with RC-CBCT. For the first five fractions the setup was according to radiographs prior to the first treatment day; thereafter, a running average over the most recent five scans was used with a 3 mm action level. Only 2/11 patients required no further correction while 9/11 required correction after the first five scans (and treatments). Two patients required further correction—one after 2 weeks of treatment, the other after two and again after

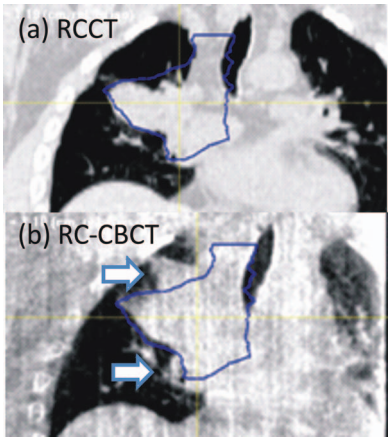

FIG. 9. Coronal section of Patient 1 in (a) the end-expiration respiration-correlated CT (RCCT) at simulation; (b) the end-expiration respiration-correlated cone-beam CT (RC-CBCT) at treatment 19 days later. Contours indicate the outline of the GTV drawn on the RCCT. Arrows in (b) indicate regions where the GTV in the cone-beam CT has grown outside the RCCT-defined GTV.

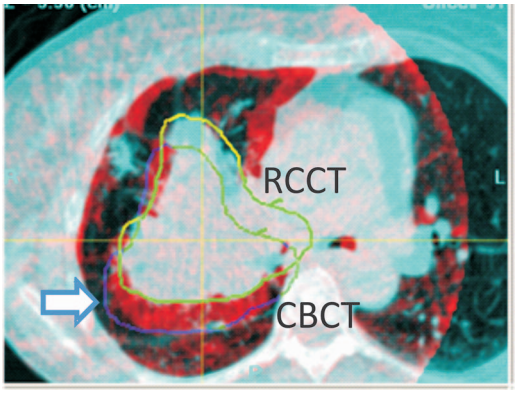

FIG. 10. Overlay of coronal sections from the respiration-correlated CT (RCCT, blue enhanced) and respiration-correlated cone-beam CT (CBCT, red) of Patient 7. The images are aligned to the vertebral column. Yellow curve indicates outline of the GTV drawn on the RCCT; blue curve indicates location in the cone-beam CT of the GTV, which has shifted 14 mm posteriorly relative to the RCCT (arrow).

3 weeks of treatment. This small study suggests a need for continued surveillance in this patient population. As an unrelated (and unexpected) finding in 2/11 cases, the first CBCT revealed that the GTV changed in the time between simulation and first treatment, leading to revised PTVs and treatment plans. These cases indicate that a single cone-beam CT can be useful for assessing gross tumor changes early in treatment, especially when more than a few days elapse between simulation and the start of treatment.

There are two additional goals of this study. The first is to use the acquired images to evaluate the effectiveness of RC-CBCT guided correction of systematic error in lung tumor position in standard fractionated radiation treatment of locally advanced NSCLC by comparison to correction schemes based on skeletal anatomy. Although the use of CBCT is increasing, such advanced methods are still unavailable to many patients and the images acquired in this protocol give a better understanding of the advantages to be gained. Our earlier study has shown that interfractional variations in lung tumor position relative to the skeletal anatomy do occur in this patient group, and that correction of systematic error in tumor position may improve treatment accuracy.[13] A second study goal is to examine whether explicit measurement of tumor respiratory motion trajectories is important to tumor localization, by comparing registration of respiration-correlated image sets to that of respiration-averaged images. Tools for acquiring respiration-averaged images are more widely available and rigid registration of respiration-averaged CT and CBCT images is a well-established and time-efficient procedure.

In the first study goal, our findings suggest that an off-line protocol to correct GTV-based systematic error in locally advanced NSCLC can be effective at reducing tumor deviations, although the findings need confirmation with larger patient statistics. GTV-based systematic (Type 1) corrections show significantly lower residual tumor position errors relative to a bony-based systematic (Type 2) correction ($p = 0.014$) and to a bony-based weekly (Type 4) correction ($p = 0.001$). Type 1 correction yields lower mean 3D residual tumor position error in 9 out of 11 cases relative to Type 2 (Fig. 6), although the difference in mean residual error between the two methods is less than 2 mm in seven of those cases. Mean residual error in Type 1 correction is lower by more than 2 mm in 6/11 cases relative to Type 4 correction. Although residual error with Type 1 correction is not significantly lower relative to daily bony-based (Type 3) correction, the former is achieved with substantially fewer measurements and corrections, with an average of 9.4 measurements and 1.1 corrections per patient (average of 27 fractions per treatment course) in this study. Noting that Type 3 corrects for both systematic and random errors in patient setup, whereas Type 1 corrects for systematic error in both setup and interfractional GTV deviations relative to bony anatomy, it is likely that correction of random setup errors in Type 3 partly compensates the advantage of Type 1 corrections. An additional consideration with radiograph-based corrections is that the images may be difficult to interpret in the presence of deformations or out-of-plane rotations, although this was not investigated in our study. It is also worth noting that most (9 out of 11) cases show small ($\leq$6 mm) respiration-induced tumor motion in the simulation RCCT. All cases have tumor attached to the mediastinum, which limits the amount of respiration-induced motion. Examination of GTV-based versus bony-based residual error shows no clear correlation with motion (Fig. 7), although there are too few cases to assess the efficacy of GTV-based correction with larger tumor motion.

We compare our results to other CBCT studies of standard fractionated treatment in lung. Yeung *et al.* have used CBCT guidance to localize lung tumors in each fraction of conventionally fractionated treatments of 13 patients.[9] They report mean $\pm$ SD differences between GTV-guided and bony-guided corrections (couch shifts) of -0.6 ± 2.4, 0.3 ± 3.1, and -1.1 ± 6.7 mm, in the LR, AP, and SI directions, respectively. In our study, the differences between GTV-aligned and bony-aligned corrections, $T_{g,i} - T_{b,i}$, $i \geq 6$, are 0.9 ± 2.9, 0.0 ± 4.1, and 1.1 ± 3.8 mm, respectively, consistent with those reported by Yeung *et al.* Juhler-Nøttrup *et al.* have examined interfractional changes in tumor volume and position with respiration-correlated CBCT, but did not perform patient corrections based on GTV-based image registration.[22] Bissonnette *et al.* have examined geometric accuracy of lung tumor localization using couch adjustment immediately following daily CBCT guidance,[10] and retrospectively analyzed RC-CBCT scans to investigate inter- and intrafractional variations in lung tumor motion amplitude.[3] Harsolia *et al.* have compared 3D-conformal treatment plans using free-breathing CT with various planning techniques that use RC-CBCT.[23] In one such technique, referred to as 4D adaptive planning with a single correction, a combination of fluoroscopy and an RC-CBCT scan is used to determine a respiratory-mean target position and provides the basis for planning. In the first five fractions, daily fluoroscopy is used to determine an estimated probability density function (PDF) of target position vs time including respiratory motion and setup deviations, which is used to adjust beam apertures in the adapted plan. The study of eight patients treated for lung cancer shows a mean decrease in PTV volume of 39% for the 4D adaptive plans,

relative to the 3D plans. Although the methodology and results of this study are not directly applicable to our findings, it is worth noting that their patient group shows larger tumor motion than our study: in the former, seven out of eight cases have tumor SI motion exceeding 6 mm (mean ± SD: 10 ± 5 mm), whereas in the latter, only 2 out of 11 cases show SI motion exceeding 6 mm (mean ± SD: 5 ± 4 mm). A possible reason for the discrepancy is that the Harsolia study required tumors to be distinctly visible in fluoroscopy used for weekly imaging, which generally excluded tumors attached to the mediastinum, in contrast to our study which used RC-CBCT throughout the treatment course and did not have such a restriction. Mediastinal involvement is common in later stage lung cancer cases.[24] Higgins *et al.* found that systematic error correction of locally advanced lung cancer based on CBCT guidance in the first five treatment days did not reduce residual errors compared to that for no image guidance.[25] Their image guidance procedure used the end-expiration image from the planning RCCT as the reference, to which a free-breathing CBCT was registered by alignment of the spine. In cases in which the visible tumor was outside of the PTV (consisting of a 5 mm CTV margin around the gross tumor in RCCT images at end inspiration and expiration, a fusion of the CTVs to form an ITV, plus a 5 mm margin), further adjustments were performed. This is in contrast to our study, in which Type 1 corrections used a 3 mm action level on respiration-averaged tumor position derived from RCCT and RC-CBCT. Our findings suggest that the particular method of determining target deviations is important to the effectiveness of protocols that correct systematic error. We further note that it is important to differentiate between conclusions obtained from advanced stage lung cancer studies such as ours and studies of early stage lung cancer hypofractionated treatments, in which the importance of daily CBCT guidance to correct for interfraction variability of tumor position has been clearly demonstrated.[3–8]

In 2/11 cases, the first CBCT revealed that the GTV changed in the time between simulation and first treatment, leading to revised PTVs and treatment plans. These cases indicate that even a single cone-beam CT can be useful for assessing gross tumor changes early in treatment, especially when more than a few days elapse between simulation and the start of treatment.

In the second study goal, our results indicate that for tumor localization of later-stage NSCLC, GTV displacements determined using respiration-averaged imaging are consistent with those from respiration-correlated imaging. Differences in the two localization methods show little correlation with tumor motion extent (Fig. 8), although more patient cases with more mobile tumors are needed to confirm this. We note that although in this study, the respiration-averaged CBCT is produced from the RC-CBCT using all projections, a standard one-minute CBCT spans typically spans 15 or more respiration cycles, thus would be sufficient for this purpose. Our findings are comparable to those of Hugo *et al.*,[26] who have found that mean discrepancy in tumor position between the respiration-averaged and respiration-correlated methods is within 1.0–1.4 mm in each of the three principal directions. Further, the discrepancies in that report are not observed to vary with the magnitude of tumor motion, consistent with our findings. Although the respiration-correlated method allows one to measure changes in respiratory motion during treatment, the respiration-averaged method is more easily implemented in the clinic and would facilitate an off-line protocol to correct GTV-based systematic error.

ACKNOWLEDGMENTS

This work was supported in part by National Cancer Institute Award Nos. T32-CA61801 and R01-CA126993, and by a research grant from Varian Medical Systems. The content is solely the responsibility of the authors and does not necessarily represent the official views of the National Cancer Institute or the National Institutes of Health. The authors thank Andrew Jeung, Hassan Mostafavi, Peter Munro, and Edward Seppi for providing assistance in cone-beam CT acquisition with patient respiration signals and providing reconstruction software.

[a]Current address: Beth Israel Medical Center, 10 Union Square East, New York, NY 10003.
[b]Current address: Department of Radiation Oncology, Mount Sinai Medical Center, New York, NY 10029.
[c]Author to whom correspondence should be addressed. Electronic mail: magerasg@mskcc.org; Telephone: 646-888-5615.

[1]RTOG0617, "A randomized phase III comparison of standard-dose (60 Gy) versus high-dose (74 Gy) conformal radiotherapy with concurrent and consolidation carboplatin paclitaxel +/− cetuximab in patients with stage IIIA/IIIB non-small cell lung cancer" (2011) (available URL: http://www.rtog.org/ClinicalTrials/ProtocolTable/StudyDetails.aspx?study=0617). Last accessed April 30, 2012.
[2]RTOG1106, "Randomized phase II trial of individualized adaptive radiotherapy using during-treatment FDG-PET/CT and modern technology in locally advanced non-small cell lung cancer (NSCLC)" (2011) (available URL: http://www.rtog.org/ClinicalTrials/ProtocolTable/StudyDetails.aspx?study=1106). Last accessed April 30, 2012.
[3]J. P. Bissonnette, K. N. Franks, T. G. Purdie, D. J. Moseley, J. J. Sonke, D. A. Jaffray, L. A. Dawson, and A. Bezjak, "Quantifying interfraction and intrafraction tumor motion in lung stereotactic body radiotherapy using respiration-correlated cone beam computed tomography," Int. J. Radiat. Oncol. Biol. Phys. **75**, 688–695 (2009).
[4]T. G. Purdie, D. J. Moseley, J. P. Bissonnette, M. B. Sharpe, K. Franks, A. Bezjak, and D. A. Jaffray, "Respiration correlated cone-beam computed tomography and 4DCT for evaluating target motion in Stereotactic Lung Radiation Therapy," Acta Oncol. **45**, 915–922 (2006).
[5]I. S. Grills, G. Hugo, L. L. Kestin, A. P. Galerani, K. K. Chao, J. Wloch, and D. Yan, "Image-guided radiotherapy via daily online cone-beam CT substantially reduces margin requirements for stereotactic lung radiotherapy," Int. J. Radiat. Oncol. Biol. Phys. **70**, 1045–1056 (2008).
[6]Z. Wang, J. W. Nelson, S. Yoo, Q. J. Wu, J. P. Kirkpatrick, L. B. Marks, and F. F. Yin, "Refinement of treatment setup and target localization accuracy using three-dimensional cone-beam computed tomography for stereotactic body radiotherapy," Int. J. Radiat. Oncol. Biol. Phys. **73**, 571–577 (2009).
[7]J. J. Sonke, M. Rossi, J. Wolthaus, M. van Herk, E. Damen, and J. Belderbos, "Frameless stereotactic body radiotherapy for lung cancer using four-dimensional cone beam CT guidance," Int. J. Radiat. Oncol. Biol. Phys. **74**, 567–574 (2009).
[8]K. Matsugi, Y. Narita, A. Sawada, M. Nakamura, Y. Miyabe, Y. Matsuo, M. Narabayashi, Y. Norihisa, T. Mizowaki, and M. Hiraoka, "Measurement of interfraction variations in position and size of target volumes in stereotactic body radiotherapy for lung cancer," Int. J. Radiat. Oncol. Biol. Phys. **75**, 543–548 (2009).
[9]A. R. Yeung, J. G. Li, W. Y. Shi, H. E. Newlin, A. Chvetsov, C. R. Liu, J. R. Palta, and K. Olivier, "Tumor localization using

cone-beam CT reduces setup margins in conventionally fractionated radiotherapy for lung tumors," Int. J. Radiat. Oncol. Biol. Phys. **74**, 1100–1107 (2009).
[10]J. P. Bissonnette, T. G. Purdie, J. A. Higgins, W. Li, and A. Bezjak, "Cone-beam computed tomographic image guidance for lung cancer radiation therapy," Int. J. Radiat. Oncol. Biol. Phys. **73**, 927–934 (2009).
[11]X. Wang, R. Zhong, S. Bai, Q. Xu, Y. Zhao, J. Wang, X. Jiang, Y. Shen, F. Xu, and Y. Wei, "Lung tumor reproducibility with active breath control (ABC) in image-guided radiotherapy based on cone-beam computed tomography with two registration methods," Radiother. Oncol. **99**, 148–154 (2011).
[12]G. X. Ding and C. W. Coffey, "Radiation dose from kilovoltage cone beam computed tomography in an image-guided radiotherapy procedure," Int. J. Radiat. Oncol. Biol. Phys. **73**, 610–617 (2009).
[13]J. Chang, G. S. Mageras, E. Yorke, F. De Arruda, J. Sillanpaa, K. E. Rosenzweig, A. Hertanto, H. Pham, E. Seppi, A. Pevsner, C. C. Ling, and H. Amols, "Observation of interfractional variations in lung tumor position using respiratory gated and ungated megavoltage cone-beam computed tomography," Int. J. Radiat. Oncol. Biol. Phys. **67**, 1548–1558 (2007).
[14]E. C. Ford, G. S. Mageras, E. Yorke, and C. C. Ling, "Respiration-correlated spiral CT: A method of measuring respiratory-induced anatomic motion for radiation treatment planning," Med. Phys. **30**, 88–97 (2003).
[15]D. A. Low, M. Nystrom, E. Kalinin, P. Parikh, J. F. Dempsey, J. D. Bradley, S. Mutic, S. H. Wahab, T. Islam, G. Christensen, D. G. Politte, and B. R. Whiting, "A method for the reconstruction of four-dimensional synchronized CT scans acquired during free breathing," Med. Phys. **30**, 1254–1263 (2003).
[16]T. Pan, T. Y. Lee, E. Rietzel, and G. T. Chen, "4D-CT imaging of a volume influenced by respiratory motion on multi-slice CT," Med. Phys. **31**, 333–340 (2004).
[17]S. S. Vedam, P. J. Keall, V. R. Kini, H. Mostafavi, H. P. Shukla, and R. Mohan, "Acquiring a four-dimensional computed tomography dataset using an external respiratory signal," Phys. Med. Biol. **48**, 45–62 (2003).
[18]T. F. Li, L. Xing, P. Munro, C. McGuinness, M. Chao, Y. Yang, B. Loo, and A. Koong, "Four-dimensional cone-beam computed tomography using an on-board imager," Med. Phys. **33**, 3825–3833 (2006).
[19]J. Lu, T. M. Guerrero, P. Munro, A. Jeung, P. C. M. Chi, P. Balter, X. R. Zhu, R. Mohan, and T. Pan, "Four-dimensional cone beam CT with adaptive gantry rotation and adaptive data sampling," Med. Phys. **34**, 3520–3529 (2007).
[20]J. J. Sonke, L. Zijp, P. Remeijer, and M. van Herk, "Respiratory correlated cone beam CT," Med. Phys. **32**, 1176–1186 (2005).
[21]S. A. Kriminski, D. M. Lovelock, V. E. Seshan, I. Ali, P. Munro, H. I. Amols, Z. Fuks, M. Bilsky, and Y. Yamada, "Comparison of kilovoltage cone-beam computed tomography with megavoltage projection pairs for paraspinal radiosurgery patient alignment and position verification," Int. J. Radiat. Oncol. Biol. Phys. **71**, 1572–1580 (2008).
[22]T. Juhler-Nottrup, S. S. Korreman, A. N. Pedersen, G. F. Persson, L. R. Aarup, H. Nystrom, M. Olsen, N. Tarnavski, and L. Specht, "Interfractional changes in tumour volume and position during entire radiotherapy courses for lung cancer with respiratory gating and image guidance," Acta Oncol. **47**, 1406–1413 (2008).
[23]A. Harsolia, G. D. Hugo, L. L. Kestin, I. S. Grills, and D. Yan, "Dosimetric advantages of four-dimensional adaptive image-guided radiotherapy for lung tumors using online cone-beam computed tomography," Int. J. Radiat. Oncol. Biol. Phys. **70**, 582–589 (2008).
[24]R. J. Ginsberg, E. E. Vokes, and K. Rosenzweig, "Non-small cell lung cancer," in *Cancer Principles and Practice of Oncology*, edited by V. T. Devita, S. Hellman, and S. A. Rosenberg (Lippincott, Philadelphia, 2001), pp. 925–983.
[25]J. Higgins, A. Bezjak, A. Hope, T. Panzarella, W. Li, J. B. C. Cho, T. Craig, A. Brade, A. Sun, and J. P. Bissonnette, "Effect of image-guidance frequency on geometric accuracy and setup margins in radiotherapy for locally advanced lung cancer," Int. J. Radiat. Oncol. Biol. Phys. **80**, 1330–1337 (2011).
[26]G. D. Hugo, J. A. Liang, J. Campbell, and D. Yan, "On-line target position localization in the presence of respiration: A comparison of two methods," Int. J. Radiat. Oncol. Biol. Phys. **69**, 1634–1641 (2007).